

Article

Electron Capture and Ionisation in Collisions of Ne^{10+} and Li^{3+} with Atomic Hydrogen

Aks M. Kotian ^{1,*}, Corey T. Plowman ¹, Ilkhom B. Abdurakhmanov ², Igor Bray ¹ and Alisher S. Kadyrov ^{1,*}

¹ Department of Physics and Astronomy and Curtin Institute for Computation, Curtin University, GPO Box U1987, Perth, WA 6845, Australia

² Pawsey Supercomputing Centre, 1 Bryce Ave., Kensington, WA 6151, Australia

* Correspondence: akshit.kotian@student.curtin.edu.au (A.M.K.); a.kadyrov@curtin.edu.au (A.S.K.)

Abstract: The two-center wave-packet convergent close-coupling method has been applied to model the processes of electron capture and ionisation in collisions of fully stripped neon and lithium ions with atomic hydrogen at projectile energies from 1 keV/u to 1 MeV/u. For the Ne^{10+} projectile, the resulting total electron-capture cross section lies between the two sets of experimental results available for system, which differ from each other significantly. For Li^{3+} , our total electron-capture cross section agrees with the available experimental measurements by Shah et al. [J. Phys. B: At. Mol. Opt. Phys 11, L233 (1978)] and Seim et al. [J. Phys. B: At. Mol. Opt. Phys 14, 3475 (1981)], particularly at low and high energies. We also get good agreement with the existing theoretical works, particularly the atomic- and molecular-orbital close-coupling calculations. Our total ionisation cross section overestimates the experimental data by Shah et al. [J. Phys. B: At. Mol. Opt. Phys 15, 413 (1982)] at the peak, however we get good agreement with the other existing theoretical calculations at low and high energies.



Citation: Kotian, A.M.; Plowman, C.T.; Abdurakhmanov, I.B.; Bray, I.; Kadyrov, A.S. Electron Capture and Ionisation in Collisions of Ne^{10+} and Li^{3+} with Atomic Hydrogen. *Atoms* **2022**, *10*, 144. <https://doi.org/10.3390/atoms10040144>

Academic Editors: Izumi Murakami, Daiji Kato, Hiroyuki A. Sakaue and Hajime Tanuma

Received: 20 October 2022

Accepted: 30 November 2022

Published: 1 December 2022

Publisher's Note: MDPI stays neutral with regard to jurisdictional claims in published maps and institutional affiliations.



Copyright: © 2022 by the authors. Licensee MDPI, Basel, Switzerland. This article is an open access article distributed under the terms and conditions of the Creative Commons Attribution (CC BY) license (<https://creativecommons.org/licenses/by/4.0/>).

Keywords: plasma physics; neon; lithium; fusion research; highly charged ion

1. Introduction

Accurate modelling of collisions between ions and atoms is particularly important in astrophysical and fusion plasma research. In tokamak fusion reactors, hydrogen atoms are typically introduced to the central plasma region of the reactor for heating and diagnostics of the plasma [1,2]. Additionally, impurity ions which have been stripped from the wall of the reactor are also present in the central plasma region. The resulting ion-atom collisions between the hydrogen atoms and impurity ions can lead to electronic excitation of the hydrogen atom or electron capture into an excited state of the impurity ion. As the electrons de-excite, they release photons of specific wavelengths and the resulting spectra can be used to measure important data, including the radial temperature profile and the density of the plasma. The charge-exchange spectroscopy (CX) technique is employed alongside beam-exchange spectroscopy (BES) diagnostics [3] to obtain these data. These diagnostic techniques, however, require accurate state-selective cross sections for target excitation and electron capture in collisions between the impurity ions and atoms present in the plasma. The two-center wave-packet convergent close-coupling method (WP-CCC) [4,5] can be used to evaluate such cross sections. Here we consider collisions of fully stripped neon and lithium ions with hydrogen that are particularly relevant to the current fusion reactors.

Experimental measurements for collisions of fully stripped neon ions with atomic hydrogen have only been performed for the total electron-capture cross section (TECS). These are the measurements by Panov et al. [6] and Meyer et al. [7] with an uncertainty of about 17%. They made measurements at energies between 0.1 and 10 keV/u, however, there is poor agreement between the two sets of data over this energy range. For collisions of fully stripped lithium ions with atomic hydrogen, experimental measurements were

performed by Shah et al. [8], Seim et al. [9] and Shah and Gilbody [10]. For Li^{q+} ions colliding with atomic hydrogen, where $q = 1, 2$ and 3 , Shah et al. [8] measured the TECS at projectile energies between 14 and 300 keV/u. Shah and Gilbody [10] performed measurements for the total ionisation cross section (TICS) at projectile energies between 50 and 400 keV/u. The TECS measurements by Shah et al. [8] have an average uncertainty of 20% and the TICS measurements by Shah and Gilbody [10] have an average uncertainty of 4.9%. Seim et al. [9] also performed measurements for the TECS at projectile energies between 1 and 6 keV/u with an average uncertainty of 15%.

A number of theoretical methods have been employed to calculate cross sections for collisions of Ne^{10+} and Li^{3+} with ground-state atomic hydrogen. These are the atomic-orbital close-coupling (AOCC) method [11–16], the continuum distorted-wave (CDW) approach [17], a hybrid of the eikonal initial-state and CDW approximations, labelled as the CDW-EIS approach [18], a three-body eikonal approach (TBEA) [19], the advanced adiabatic (AA) method [20], the molecular orbital close-coupling (MOCC) approach [21], the classical trajectory Monte Carlo (CTMC) method [21–23], the boundary-corrected continuum intermediate states (BCIS) method [24] and the two-center basis generator method (TC-BGM) [25]. For the TECS, the primary discrepancy present within the existing theoretical methods is the disagreement between the hydrogenic CTMC (hCTMC) results [21] and the older CTMC calculations, including the microcanonical CTMC (mCTMC) calculations [21]. For the TICS, however, none of the existing theoretical calculations are in good agreement with the available experimental data.

The WP-CCC method [4,5] has been employed to calculate cross sections for various ion-atom collisional systems over a wide energy range. These collisional processes include protons incident on atomic [26,27] and molecular hydrogen [28,29], multiply charged ion projectiles incident on atomic targets [30–33] and proton collisions with helium [34–36]. In this work we aim to perform similar calculations for $\text{Ne}^{10+} - \text{H}(1s)$ and $\text{Li}^{3+} - \text{H}(1s)$ collisions over a wide energy range from 1 to 1000 keV/u and provide the electron-capture and ionisation cross sections.

2. Details of the WP-CCC Method

Here we provide a brief overview of the WP-CCC method. The details of the theory have been given in [5,31,33].

In a semiclassical approximation, the trajectory of the projectile can be written as $\mathbf{R} = \mathbf{b} + \mathbf{v}t$, where \mathbf{R} is the projectile's position relative to the target nucleus, \mathbf{b} is the impact parameter, \mathbf{v} is the incident velocity of the projectile and t is time. For the system at hand, we solve the full three-body Schrödinger equation. This is done by substituting a two-center expansion of the total scattering wave function in a basis of square-integrable functions (including pseudostates that discretise the continuum) into the Schrödinger equation. Applying the semiclassical approximation then yields a set of coupled first-order differential equations for the time-dependent expansion coefficients, which are then solved computationally. Further details can be found in [33].

The probability of a specific transition, $P(b)$, can be written as the expansion coefficient's magnitude square as $t \rightarrow +\infty$. The cross section for the transition is then obtained by integrating the weighted probability, $bP(b)$, over all the impact parameters. From this, the TECS is given by the sum of the partial cross sections for capture into negative-energy states on the projectile. Similarly, the TICS is given by the sum of the partial cross sections for capture into positive-energy states on the projectile and target.

The details of the calculations for the Ne^{10+} projectile have been given in [33]. Here, we briefly detail the parameters that are different for the $\text{Li}^{3+} - \text{H}(1s)$ calculations. The size of the target and projectile bases used in close-coupling calculations determine the accuracy of the results. The bases, themselves, depend on the parameters such as the maximum principle quantum number of the bound states, n_{max} , the maximum angular momentum quantum number, l_{max} , and the number of continuum pseudostates, N_c . Thus, it is important to establish convergence in all of the presented cross sections with respect to the basis

parameters in order to make sure that the results are reliable and accurate. We reached convergence in the TECS and TICS to within 1% by using a symmetric basis with $n_{\max} = 10$, $l_{\max} = 5$ and $N_c = 20$.

In our cross-section calculations, the weighted probability is integrated up to a large enough impact parameter, b_{\max} , beyond which the weighted probabilities are negligible. The choice of b_{\max} is dependent on the projectile energy. At low projectile energies, $b_{\max} = 18$ a.u. was found to be sufficient for the weighted total electron-capture probability to fall off sufficiently from its peak to ensure that the integration is done accurately. The weighted total electron-capture probability falls off a lot more sharply at higher energies, but the weighted ionisation probability falls off not as fast. Thus, at the higher impact energies, b_{\max} had to be as large as 56 a.u. in order to get reliable TICS. The ejected-electron energy is also truncated at a sufficiently large ϵ_{\max} , beyond which the contribution from the continuum towards the TICS is negligible. At the lowest incident energy considered in this work (1 keV/u), $\epsilon_{\max} = 20$ eV was sufficient. However, the value of ϵ_{\max} required to obtain converged results for the TICS increases with the impact energy. So, at 1 MeV/u (the highest considered in this work) we had to set $\epsilon_{\max} = 1000$ eV. We also note that at the impact energy of 90 keV/u, where the TICS peaks, $\epsilon_{\max} = 300$ eV was required.

3. Results and Discussion

3.1. The Ne^{10+} Projectile

In Figure 1, we plot the calculated TECS for $Ne^{10+} - H(1s)$ collisions alongside previous theoretical calculations and experimental measurements. It is customary to use a logarithmic scale to represent the TECS as it falls off by several orders of magnitude as a function of energy. The left panel shows a wide energy region using the logarithmic scale. The right panel highlights the low- and intermediate-energy regions using the linear scale. Below the projectile energy of 10 keV/u, the present results are in agreement with the MOCC [21] results. Our results are in good agreement with the hCTMC [21] and AOCC [13,16] results over the entire 1–1000 keV/u energy range. Though they are somewhat lower than the older CTMC calculations [21–23], we do get good agreement with the latest hCTMC calculations by Errea et al. [21]. As one can see our results lie between the experimental measurements by Meyer et al. [7] and Panov et al. [6], which differ from each other significantly. Considering that multiple sets of theoretical calculations (except the older CTMC ones) are in agreement at low energies suggests that there could be some systematic uncertainty present in the available experimental data.

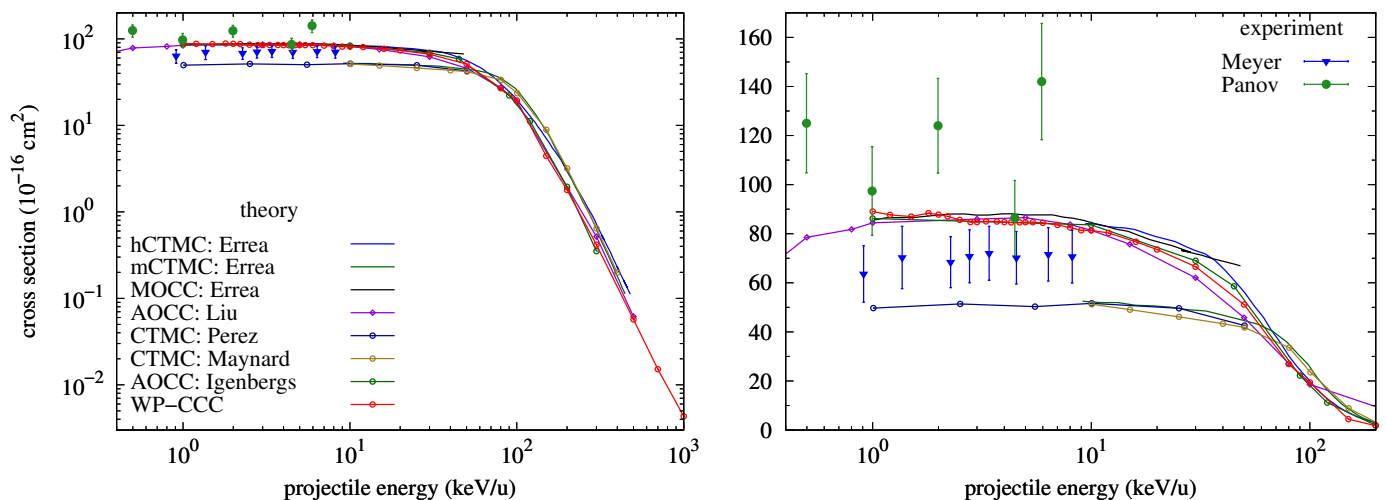


Figure 1. The total cross section for electron capture in $Ne^{10+} - H(1s)$ collisions calculated using the WP-CCC method. Experimental measurements are by Panov et al. [6] and Meyer et al. [7]. Also included

are the MOCC calculations by Errea et al. [21], the AOCC calculations by Igenbergs [13] and Liu et al. [16] and the CTMC calculations by Errea et al. [21], Perez et al. [23] and Maynard et al. [22]. The left panel shows a wide energy region using the logarithmic scale. The right panel highlights the low- and intermediate-energy regions using the linear scale. The keys shown in the left and right panels apply to both panels. The left panel was first published in Ref. [33] and reproduced in compliance with IOP's Author Rights Policy.

3.2. The Li^{3+} Projectile

In Figure 2, we plot the calculated TECS for $\text{Li}^{3+} - \text{H}(1s)$ collisions alongside the existing experimental data and other theoretical calculations. We find good agreement with both sets of experimental data [8,9], which span most of the energy range considered in this work. Our results are somewhat higher than the experimental measurements by Shah et al. [8] at intermediate energies, which, however, is the case for most of the available theoretical methods. We get good agreement with both sets of the CTMC results by Errea et al. [21] at high energies. The microcanonical distribution for the initial electron cloud yields a spatial density which is too compact, whereas the hydrogenic distribution provides a better representation of the spatial density. Therefore, the hCTMC method is expected to be more reliable than the mCTMC one. Nevertheless, at intermediate energies, the hCTMC results are also larger than the experimental measurements by Shah et al. [8]. Furthermore, within this energy region, the hCTMC calculations are in poor agreement with the MOCC ones by the same authors. Fritsch and Lin [11] calculated the TECS at low energies using the AOCC approach, however, the size of their basis was too small to give convergent results. The AA calculations by Janev et al. [20] are also available only at low energies. Both sets of results disagree with the experimental measurements by Seim et al. [9] and the other theoretical calculations available at these energies, including ours. The TBEA calculations by Alt et al. [19] disagree with both sets of experimental measurements over the entire energy range. In their calculations, Alt et al. [19] neglected the second- and higher-order terms in the quasi-Born expansion of their effective potential. This was suggested as a possible reason for disagreement with the experimental data. Our calculations are in good agreement with the TC-BGM results by Leung and Kirchner [25] and the AOCC results by Liu et al. [14] over the entire 1–1000 keV/u energy range. The CDW calculations by Datta et al. [17] and the BCIS calculations by Delibašić et al. [24] significantly overestimate the data at intermediate energies, but we get better agreement at high energies. This is as expected, since both methods are perturbative approaches and very accurate at sufficiently high energies. Overall, the present results are in excellent agreement with the experimental data at low and high energies with slight disagreement near the peak of the cross section.

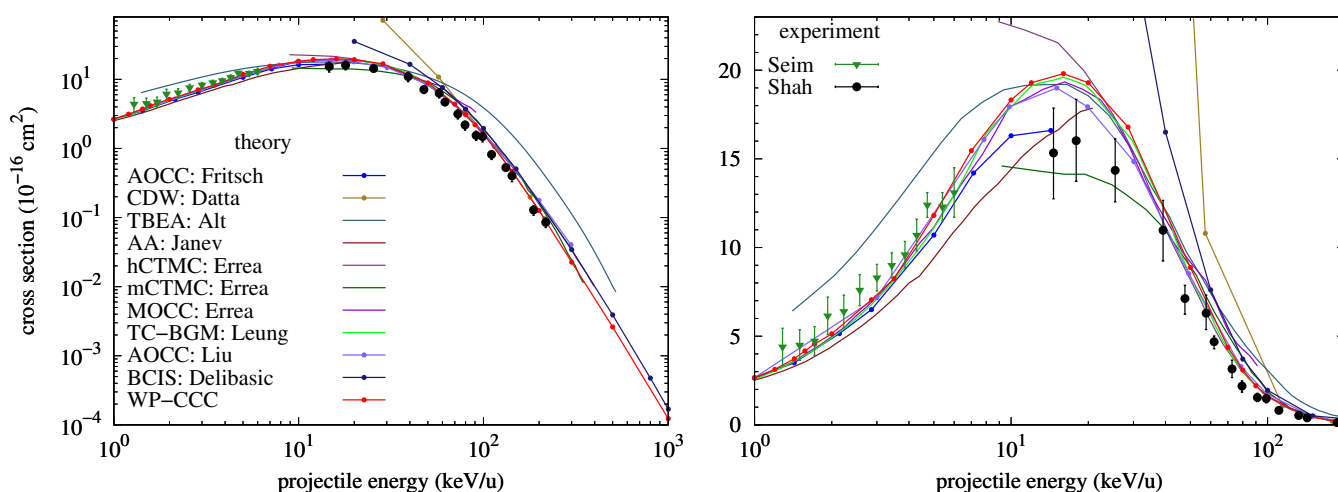


Figure 2. The total cross section for electron capture in $\text{Li}^{3+} - \text{H}(1s)$ collisions calculated using the WP-CCC method. Experimental measurements are by Shah et al. [8] and Seim et al. [9]. Also included

are the AOCC calculations by Fritsch and Lin [11], CDW calculations by Datta et al. [17], TBEA calculations by Alt et al. [19], AA calculations by Janev et al. [20], hCTMC, mCTMC and MOCC calculations by Errea et al. [21], TC-BGM calculations by Leung and Kirchner [25], AOCC calculations by Liu et al. [14] and BCIS calculations by Delibašić et al. [24]. The left panel shows a wide energy region using the logarithmic scale. The right panel highlights the low- and intermediate-energy regions using the linear scale. The keys shown in the left and right panels apply to both panels.

We have also calculated nl -partial electron-capture cross sections, where n and l are the final-state principal and orbital angular momentum quantum numbers, respectively. In Figure 3, we plot the partial cross sections for electron capture into $2l$ and $3l$ states in collisions of fully stripped lithium ions with atomic hydrogen. We present results for these states in particular because we find that capture into these states have the largest contribution towards the TECS. Noticeable oscillations are observed in the $3s$ electron-capture cross section at low energies. However, since the magnitude of this cross section is small compared to the $2l$ and the other $3l$ electron-capture cross sections, these oscillations are not visible in the TECS. Generally, this oscillatory behaviour is seen in all n and nl cross sections for $n > 3$ as well. Similar oscillations were seen in the state-selective cross sections for capture into states with $n \geq 8$ in fully stripped neon-ion collisions with atomic hydrogen and discussed in further detail in [33].

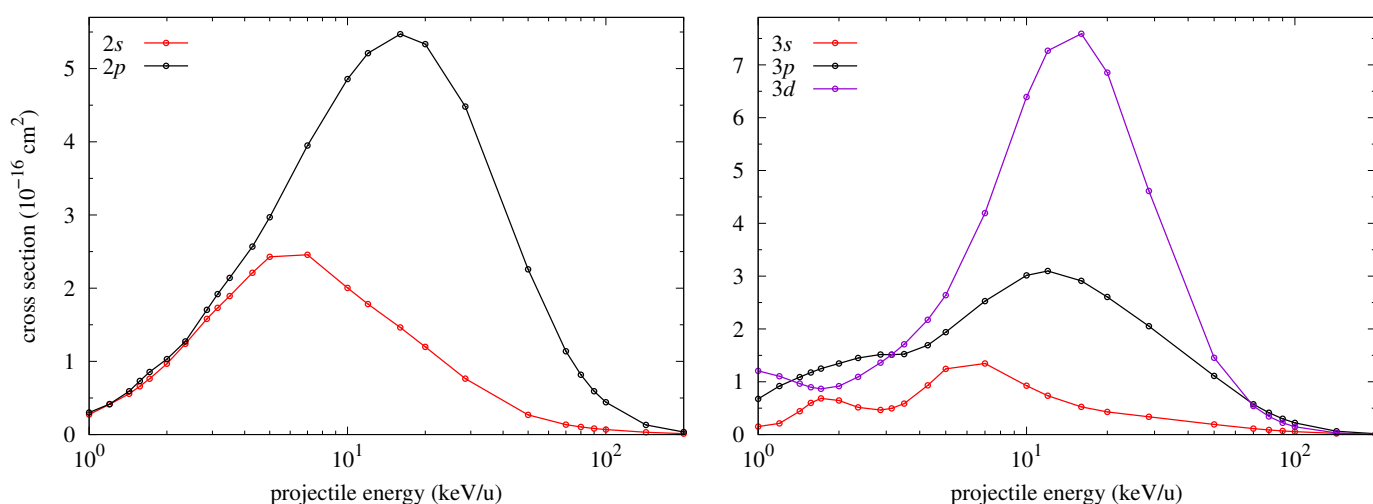


Figure 3. The $2l$ and $3l$ electron-capture cross sections for $\text{Li}^{3+}-\text{H}(1s)$ collisions over the projectile energy range from 1 to 300 keV/u.

In Figure 4 we present our calculated TICS alongside the existing experimental data by Shah and Gilbody [10] and previous theoretical results. We observe that our calculations overestimate the experimental measurements, especially in the region of the peak. Though the AOCC and TC-BGM calculations appear to better agree with the experiment, it is unclear if these cross sections are convergent in terms of the included states given that our smaller-size, i.e., non-convergent, calculations (not shown) also appear to better agree with the experiment.

The WP-CCC results lie between the hCTMC and mCTMC calculations over the entire energy range under consideration. At low energies the AA calculations by Janev et al. [20] and the AOCC calculations by Toshima [37] are quite similar to the MOCC calculations by Errea et al. [21] but our results appear to be smaller. However, at these energies, we get good agreement with the AOCC calculations by Agueny et al. [15] and the TC-BGM calculations by Leung and Kirchner [25]. The AA and MOCC methods are expected to be reliable at low energies since they incorporate molecular features. The AOCC and TC-BGM calculations are the most recent set of calculations performed for this system. All the aforementioned calculations peak at practically the same projectile energy, however, the respective peaks have different magnitudes. The CDW-EIS calculations by Crothers and

McCann [18] underestimate the TICS at intermediate energies, but we get good agreement with their calculations at high energies. More experimental measurements at intermediate energies could help resolve the disparity between the theoretical methods.

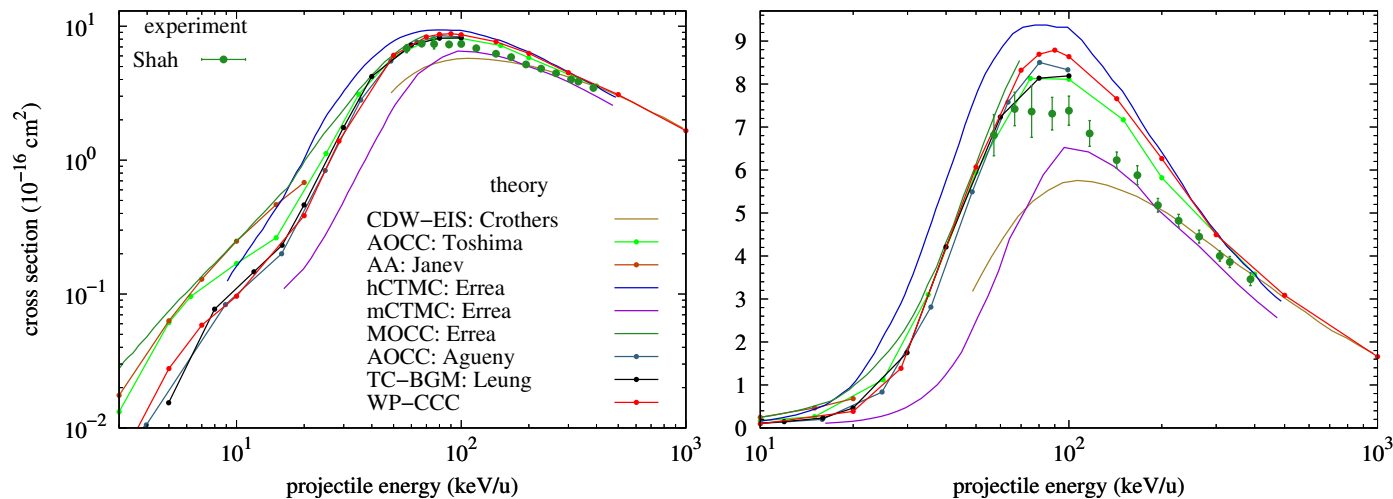


Figure 4. The total cross section for ionisation in $\text{Li}^{3+}-\text{H}(1s)$ collisions as a function of the projectile energy. The present WP-CCC results are compared with the CDW-EIS calculations by Crothers and McCann [18], AOCC calculations by Toshima [37], AA calculations by Janev et al. [20], hCTMC, mCTMC and MOCC calculations by Errea et al. [21], AOCC calculations by Agueny et al. [15] and TC-BGM calculations by Leung and Kirchner [25]. The experimental data are by Shah and Gilbody [10]. The left panel shows a wide energy region using the logarithmic scale. The right panel highlights the low- and intermediate-energy regions using the linear scale. The keys shown in the left panel apply to both panels.

4. Conclusions

We used the two-center wave-packet convergent close-coupling approach to model the processes of electron capture into the bound states of the projectile and ionisation in Ne^{10+} and Li^{3+} collisions with ground-state atomic hydrogen at impact energies between 1 and 1000 keV/u. A symmetric basis employed in this work was found to be sufficient for convergence to within 1% in the reported cross sections for $\text{Li}^{3+}-\text{H}(1s)$ collisions. However, for the neon projectile, we had to use an asymmetric basis in order for the results to converge within a few percent. Overall, for the TECS, we get very good agreement with the experimental data. For $\text{Ne}^{10+}-\text{H}(1s)$ collisions, our results lie between the experimental measurements by Panov et al. [6] and Meyer et al. [7]. Our TICS for $\text{Li}^{3+}-\text{H}(1s)$ collisions overestimates the experimental measurements by Shah and Gilbody [10] at the peak, however, we get good agreement with most of the existing theoretical calculations at low and high projectile energies. Pronounced oscillations were observed in the state-selective cross sections for capture into states with $n \geq 3$ in $\text{Li}^{3+}-\text{H}(1s)$ collisions.

The data calculated in this work is useful for fusion plasma research and can be used to aid diagnostic and spectroscopic techniques applied to model plasma with neon and lithium impurities. This work was part of the Coordinated Research Project on Data for Atomic Processes of Neutral Beams in Fusion Plasma [38] carried out under the sponsorship of the International Atomic Energy Agency.

Author Contributions: A.M.K., I.B.A. and A.S.K. developed the underlying theoretical techniques. A.M.K., C.T.P. and I.B.A. developed the code. A.M.K. performed the calculations and gathered data. A.S.K. conceptualised and supervised the project. A.M.K. and A.S.K. wrote the manuscript. C.T.P., I.B.A. and I.B.A. read and commented on the manuscript. All authors have agreed to the published version of the manuscript.

Funding: This research received no external funding.

Data Availability Statement: All the data reported in this work, as well a comprehensive set of state-selective cross sections will be available through the IAEA data repositories. In addition, these are available on reasonable request from the author.

Acknowledgments: This work was supported by the Australian Research Council, the Pawsey Supercomputer Centre, and the National Computing Infrastructure. C.T.P. acknowledges support through an Australian Government Research Training Program Scholarship. This work was part of the Coordinated Research Project carried out under the sponsorship of the International Atomic Energy Agency.

Conflicts of Interest: The authors declare no conflict of interest.

References

1. Janev, R.K. Metallic Impurities in Fusion Plasmas. *Phys. Scr.* **1991**, *T37*, 5. [[CrossRef](#)]
2. Marchuk, O. The status of atomic models for beam emission spectroscopy in fusion plasmas. *Phys. Scr.* **2014**, *89*, 114010. [[CrossRef](#)]
3. Isler, R.C. An overview of charge-exchange spectroscopy as a plasma diagnostic. *Plasma Phys. Control. Fusion* **1994**, *36*, 171. [[CrossRef](#)]
4. Abdurakhmanov, I.B.; Kadyrov, A.S.; Bray, I. Wave-packet continuum-discretization approach to ion-atom collisions: Nonrearrangement scattering. *Phys. Rev. A* **2016**, *94*, 022703. [[CrossRef](#)]
5. Abdurakhmanov, I.B.; Bailey, J.J.; Kadyrov, A.S.; Bray, I. Wave-packet continuum-discretization approach to ion-atom collisions including rearrangement: Application to differential ionization in proton-hydrogen scattering. *Phys. Rev. A* **2018**, *97*, 032707. [[CrossRef](#)]
6. Panov, M.N.; Basalae, A.A.; Lozhkin, K.O. Interaction of Fully Stripped, Hydrogenlike and Heliumlike C, N, O, Ne and Ar Ions with H and He Atoms and H₂ Molecules. *Phys. Scr.* **1983**, *T3*, 124. [[CrossRef](#)]
7. Meyer, F.W.; Howald, A.M.; Havener, C.C.; Phaneuf, R.A. Low-energy total-electron-capture cross sections for fully stripped and H-like projectiles incident on H and H₂. *Phys. Rev. A* **1985**, *32*, 3310. [[CrossRef](#)]
8. Shah, M.B.; Goffe, T.V.; Gilbody, H.B. Electron capture and loss by fast lithium ions in H and H₂. *J. Phys. B At. Mol. Phys.* **1978**, *11*, L233–L236. [[CrossRef](#)]
9. Seim, W.; Muller, A.; Wirkner-Bott, I.; Salzborn, E. Electron capture by Liⁱ⁺ (*i* = 2, 3), Nⁱ⁺ and Neⁱ⁺ (*i* = 2, 3, 4, 5) ions from atomic hydrogen. *J. Phys. B At. Mol. Phys.* **1981**, *14*, 3475–3491. [[CrossRef](#)]
10. Shah, M.B.; Gilbody, H.B. Experimental study of the ionisation of atomic hydrogen by fast lithium ions. *J. Phys. B At. Mol. Phys.* **1982**, *15*, 413–421. [[CrossRef](#)]
11. Fritsch, W.; Lin, C.D. Electron transfer in Li³⁺ + H collisions at low and intermediate energies. *J. Phys. B At. Mol. Phys.* **1982**, *15*, L281–L287. [[CrossRef](#)]
12. Tushima, N.; Tawara, H. *Excitation, Ionization, and Electron Capture Cross Sections of Atomic Hydrogen in Collisions with Multiply Charged Ions*; Technical Report; National Institute for Fusion Science: Gifu, Japan, 1995; NIFS-DATA–26.
13. Igenbergs, K. Calculations of Cross Sections Relevant for Diagnostics of Hot Fusion Plasmas. Ph.D. Thesis, Vienna University of Technology, Vienna, Austria, 2011.
14. Liu, L.; Li, X.Y.; Wang, J.G.; Janev, R.K. Cross sections for electron capture and excitation in collisions of Li_q⁺ (*q* = 1, 2, 3) with atomic hydrogen. *Phys. Plasmas* **2014**, *21*, 062513. [[CrossRef](#)]
15. Agueny, H.; Hansen, J.; Dubois, A.; Makhoute, A.; Taoutioui, A.; Sisourat, N. Electron capture, ionization and excitation cross sections for keV collisions between fully stripped ions and atomic hydrogen in ground and excited states. *At. Data Nucl. Data Tables* **2019**, *129–130*, 101281. [[CrossRef](#)]
16. Liu, L.; Wu, Y.; Wang, J.; Janev, R. Total and subshell-selective charge exchange cross sections in collisions of highly-charged Ne ions with atomic hydrogen. *At. Data Nucl. Data Tables* **2021**, *143*, 101464. [[CrossRef](#)]
17. Datta, S.; Mandal, C.R.; Mukherjee, S.C.; Sil, N.C. Calculation of cross sections for electron capture by fast Li³⁺ ions from atomic hydrogen in the continuum distorted-wave approximation. *Phys. Rev. A* **1982**, *26*, 2551–2566. [[CrossRef](#)]
18. Crothers, D.S.F.; McCann, J.F. Ionisation of atoms by ion impact. *J. Phys. B At. Mol. Phys.* **1983**, *16*, 3229–3242. [[CrossRef](#)]
19. Alt, E.O.; Avakov, G.V.; Blokhintsev, L.D.; Kadyrov, A.S.; Mukhamedzhanov, A.M. Charge-exchange reactions in a three-body eikonal approach. *J. Phys. B At. Mol. Opt. Phys.* **1994**, *27*, 4653–4674. [[CrossRef](#)]
20. Janev, R.K.; Solov'ev, E.A.; Wang, Y. Electron capture, excitation and ionization in slow collisions of ions with ground-state and metastable hydrogen atoms. *J. Phys. B At. Mol. Opt. Phys.* **1996**, *29*, 2497–2514. [[CrossRef](#)]
21. Errea, L.F.; Illescas, C.; Méndez, L.; Pons, B.; Riera, A.; Suárez, J. Classical and semi-classical treatments of Li³⁺, Ne¹⁰⁺ + H(1s) collisions. *J. Phys. B At. Mol. Opt. Phys.* **2004**, *37*, 4323. [[CrossRef](#)]
22. Maynard, G.; Janev, R.K.; Katsonis, K. Electron capture and ionization in collisions of multicharged neon ions with atomic hydrogen. *J. Phys. B At. Mol. Opt. Phys.* **1992**, *25*, 437. [[CrossRef](#)]
23. Perez, J.; Olson, R.; Beiersdorfer, P. Charge transfer and X-ray emission reactions involving highly charged ions and neutral hydrogen. *J. Phys. B At. Mol. Opt. Phys.* **2001**, *34*, 3063. [[CrossRef](#)]

24. Delibašić, D.; Milojević, N.; Mančev, I.; Belkić, D. Electron transfer from atomic hydrogen to multiply-charged nuclei at intermediate and high energies. *At. Data Nucl. Data Tables* **2021**, *139*, 101417. [[CrossRef](#)]
25. Leung, A.C.K.; Kirchner, T. Two-Center Basis Generator Method Calculations for Li^{3+} , C^{3+} , and O^{3+} , Ion Impact on Ground State Hydrogen. *Atoms* **2022**, *10*, 11. [[CrossRef](#)]
26. Abdurakhmanov, I.B.; Erkilic, O.; Kadyrov, A.S.; Bray, I.; Avazbaev, S.K.; Mukhamedzhanov, A.M. Balmer emission induced by proton impact on atomic hydrogen. *J. Phys. B At. Mol. Opt. Phys.* **2019**, *52*, 105701. [[CrossRef](#)]
27. Abdurakhmanov, I.B.; Alladustov, S.U.; Bailey, J.J.; Kadyrov, A.S.; Bray, I. Proton scattering from excited states of atomic hydrogen. *Plasma Phys. Control. Fusion* **2018**, *60*, 095009. [[CrossRef](#)]
28. Plowman, C.T.; Abdurakhmanov, I.B.; Bray, I.; Kadyrov, A.S. Effective one-electron approach to proton collisions with molecular hydrogen. *Eur. Phys. J. D* **2022**, *76*, 31. [[CrossRef](#)]
29. Plowman, C.T.; Abdurakhmanov, I.B.; Bray, I.; Kadyrov, A.S. Differential scattering in proton collisions with molecular hydrogen. *Eur. Phys. J. D* **2022**, *76*, 129. [[CrossRef](#)]
30. Faulkner, J.; Abdurakhmanov, I.B.; Alladustov, S.U.; Kadyrov, A.S.; Bray, I. Electron capture, excitation and ionization in $\text{He}^{2+} - \text{H}$ and $\text{H}^+ - \text{He}^+$ collisions. *Plasma Phys. Control. Fusion* **2019**, *61*, 095005. [[CrossRef](#)]
31. Abdurakhmanov, I.B.; Massen-Hane, K.; Alladustov, S.U.; Bailey, J.J.; Kadyrov, A.S.; Bray, I. Ionization and electron capture in collisions of bare carbon ions with hydrogen. *Phys. Rev. A* **2018**, *98*, 062710. [[CrossRef](#)]
32. Antonio, N.W.; Plowman, C.T.; Abdurakhmanov, I.B.; Bray, I.; Kadyrov, A.S. Integrated total and state-selective cross sections for bare beryllium ion collisions with atomic hydrogen. *J. Phys. B At. Mol. Opt. Phys.* **2021**, *54*, 175201. [[CrossRef](#)]
33. Kotian, A.M.; Plowman, C.T.; Abdurakhmanov, I.B.; Bray, I.; Kadyrov, A.S. State-selective electron capture in collisions of fully stripped neon ions with ground-state hydrogen. *J. Phys. B At. Mol. Opt. Phys.* **2022**, *55*, 115201. [[CrossRef](#)]
34. Alladustov, S.U.; Abdurakhmanov, I.B.; Kadyrov, A.S.; Bray, I.; Bartschat, K. Wave-packet continuum-discretization approach to proton collisions with helium. *Phys. Rev. A* **2019**, *99*, 052706. [[CrossRef](#)]
35. Spicer, K.H.; Plowman, C.T.; Abdurakhmanov, I.B.; Kadyrov, A.S.; Bray, I.; Alladustov, S.U. Differential study of proton-helium collisions at intermediate energies: Elastic scattering, excitation, and electron capture. *Phys. Rev. A* **2021**, *104*, 032818. [[CrossRef](#)]
36. Spicer, K.H.; Plowman, C.T.; Abdurakhmanov, I.B.; Alladustov, S.U.; Bray, I.; Kadyrov, A.S. Proton-helium collisions at intermediate energies: Singly differential ionization cross sections. *Phys. Rev. A* **2021**, *104*, 052815. [[CrossRef](#)]
37. Toshima, N. Coupled-channel study of collision processes involving highly-charged ions. *Phys. Scr.* **1997**, *T73*, 144–148. [[CrossRef](#)]
38. IAEA Coordinated Research Project: Data for Atomic Processes of Neutral Beams in Fusion Plasma. Available online: <https://amdis.iaea.org/CRP/neutral-beams> (accessed on 1 October 2022).